Composition Profile of PLT Films on YSZ-Buffered (100)InP

E. Vasco,* O. Böhme, E. Román, and C. Zaldo

Instituto de Ciencia de Materiales de Madrid, Consejo Superior de Investigaciones Científicas, Cantoblanco, 28049 Madrid, Spain

A. Kling and M. F. da Silva

Instituto Tecnológico e Nuclear, Estrada Nacional No. 10, 2685 Sacavém, Portugal, and Centro de Física Nuclear da Universidade de Lisboa, 1649-003 Lisboa, Portugal

Received October 12, 2000. Revised Manuscript Received December 11, 2000

The composition and interdiffusion profiles of ⟨100/001⟩-oriented (Pb,La)TiO_3 films deposited on ⟨100⟩{100}YSZ||⟨100⟩{100}InP by pulsed laser deposition have been studied by X-ray photoelectron spectroscopy and Rutherford backscattering spectroscopy. These studies demonstrate the presence of a Pb-rich region in the first 10−20 nm below the film surface, which consists of an oxygen-chemisorbed lead and (Pb,La)TiO_3 mixture. The Pb surface enrichment was clearly distinguished from the lead preferential sputtering also present. Underneath the small surface region, the film has a uniform composition close to that of the piezoelectric $Pb_{0.82}La_{0.12}TiO_3$. The PLT/YSZ and YSZ/InP interfaces are much narrower than the YSZ thickness used (≈150−200 nm). Thus, the YSZ buffer layer avoids Pb/In interdiffusion and deep reoxidation of InP and enhances the PLT orientation. This allows the integration of piezoelectric PLT on InP.

Introduction

La-modified $PbTiO_3$ ($Pb_{1-1.5x}La_xTiO_3$; PLT) is an intensively studied material with piezoelectric,[1] ferroelectric,[2,3] pyroelectric,[4] and electrooptical[5,6] applications. The physical properties of PLT are closely related to the La composition (x), which determines the tetragonality (c/a) of the crystalline structure.[7] Thus, x can be chosen in order to improve its functional properties required for specific applications: For $x = 0.15$, a large piezoelectric coefficient (d_{33} = 83.8 pm/V) has been found,[1] while at $x \approx 0.1$, the pyroelectric properties[8] and the optical losses[9] are optimized. With respect to micro- and optoelectronic applications, the integration of PLT on semiconductors is of growing relevance. PLT has been deposited on Pt/Ti/SiO_2/(100)Si,[2,10,11] $SrRuO_3$ or $LaNiO_3$/Pt/Si,[4,12] $La_{0.5}Sr_{0.5}CoO_3$/Pt/Ti/SiO_2/(100)Si,[13] $SrTiO_3$/Si,[14] Ir/Si,[11] and (100)InP.[15]

The interest in the integration of PLT on the latter material is due to the prime relevance of InP for the implementation of optoelectronic monolithic circuits in the 1.3 and 1.5 μm infrared windows, which are used in long-distance telecommunications. While diode lasers,[16] optical waveguides,[17] and phototransistors[18] are well developed on InP by growing $In_{1-0.47x}Ga_{0.47x}As_xP_{1-x}$ (x = 0−1) alloys,[19] light modulation for signal processing profits from acoustooptic interactions, for which a good piezoelectric medium (like PLT transducers) is required.

Among the $PbTiO_3$-modified structural characteristics, which determine the functional material properties, the film stoichiometry is maybe the most uncertain and difficult to control. In this context, Pb incorporation in the film is an important issue because this is the most volatile component and it is very sensitive to the deposition conditions: In pulsed laser deposition (PLD), Pb loss is observed at high substrate temperature and

* To whom correspondence should be addressed. E-mail: evasco@icmm.csic.es.

(1) Garcia, D.; Eiras, J. A. *Ferroelectrics* **1991**, *123*, 51.
(2) Rao, G. M.; Krupanidhi, S. B. *Appl. Phys. Lett.* **1994**, *64* (12), 1591.
(3) Maiwa, H.; Ichinose, N. *Jpn. J. Appl. Phys., Part 1* **1996**, *35* (9B), 4976.
(4) Tseng, Y.; Liu, K.; Jiang, J.; Lin, I. *Appl. Phys. Lett.* **1998**, *72* (25), 3285.
(5) Adachi, H.; Kawaguchi, T.; Setsune, K.; Ohji, K.; Wasa, K. *Appl. Phys. Lett.* **1983**, *42*, 867.
(6) Koo, J.; Lee, C.; No, K.; Bae, B. *Mater. Res. Soc. Symp. Proc.* **1977**, *474*, 61.
(7) Hennings, D. *Mater. Res. Bull.* **1971**, *6*, 329.
(8) Wang, C.; Chen, Y.; Lee, M.; Chiou, C.; Huang, Y. *Jpn. J. Appl. Phys., Part 1* **1999**, *38* (5A), 2831.
(9) Kang, Y. M.; Baik, S. *J. Mater. Res.* **1999**, *13* (4), 995.
(10) Yeh, M. H.; Liu, K. S.; Lin, I. N. *J. Mater. Res.* **1994**, *9* (9), 2379.
(11) Grill, A.; Laibowitz, R.; Beach, D.; Neumayer, D.; Duncobe, P. R. *Integr. Ferroelectr.* **1997**, *14* (1), 211.
(12) Tseng, Y. K.; Liu, K.; Jiang, J.; Lin, I. *Jpn. J. App. Phys., Part 1* **1998**, *37* (8), 6552.
(13) Wang, J. P.; Ling, Y. C.; Tseng, Y. K.; Liu, K. S.; Lin, I. N. *J. Mater. Res.* **1998**, *13* (5), 1286.
(14) Wang, J. P.; Ling, Y. C.; Yeh, M. H.; Li, K. S.; Lin, I. N. *Appl. Phys. Lett.* **1996**, *68* (24), 3401.
(15) Vasco, E.; Vazquez, L.; Zaldo, C. *Appl. Phys. A* **1999**, *69* (S), S827.
(16) Paraire, N. A.; Moresmau, N. S.; Chen, F.; Dansas, P.; Bertrand, F. *Appl. Opt.* **1997**, *36* (12), 2545.
(17) Sugo, M.; Mori, H.; Tachikawa, M.; Itoh, Y.; Yamamoto, M. *Appl. Phys. Lett.* **1990**, *57* (6), 593.
(18) Keavney, C. J.; Vernon, S. M.; Haven, V. E.; Wojtczuk, S. J.; Al-Jassim, M. M. *Appl. Phys. Lett.* **1989**, *54* (12), 1139.
(19) Adachi, S. *J. Appl. Phys.* **1982**, *53*, 5863.

10.1021/cm001198p CCC: $20.00 © 2001 American Chemical Society
Published on Web 02/23/2001

low deposition pressures,[20,21] while in diode sputtering the high pressure may reduce the Pb transport to the film.[22] The oxidation state of lead is often considered to be responsible for this effect,[23] because PbO has a lower vapor pressure than metallic Pb. Pb-rich targets along with high oxygen pressures during deposition are often used in PLD to compensate the lead loss. At the same time, to avoid an excess of incorporated Pb, the deposition conditions must be accurately controlled. Excessive Pb incorporation, which is segregated in the form of PbO, would be harmful for electrical applications.[24] It produces a poor ferroelectric response due to the presence of paraelectric and metallic phases, ferroelectric domain pinning, and space charge induced electric bias fields.

Although, while using the adequate deposition conditions to obtain the required PLT bulk composition, further deviations of the composition may occur at the film/substrate or film/electrode interfaces as well as at the film surface. In particular, a Pb-enriched near-surface region frequently appears in $PbTiO_3$-modified films deposited by different techniques such as sputtering,[25,26] chemical vapor deposition,[27] and sol−gel.[28,29] The surface lead enrichment modifies the ferroelectric and piezoelectric responses of the film in forming a superficial dead (nonferroelectric) layer, which is especially harmful for devices with both metallic contacts on top of the films, such as interdigital transducers used in the SAW devices.

The nature of this lead-enriched near-surface region is still controversially discussed,[28,30] because of the experimental difficulties to quantify the compositional depth profiles. So far, the composition profiles of $PbTiO_3$-modified films, studied by X-ray photoelectron spectroscopy (XPS),[28,30] secondary-ion mass spectrometry (SIMS),[31] atomic emmission spectroscopy (AES),[25,27] and Rutherford backscattering spectroscopy (RBS)[28,32] cannot elucidate unambiguously the film composition near the surface. In particular, in profiling studies based on film eroding, the constituent elements of $PbTiO_3$-modified ceramics have different sputtering yields, which also depend on the sputtering conditions. Especially, a preferential Pb sputtering is observed.[25,33] Therefore, this profiling method has not so far provided conclusive evidence of whether the measured Pb enrichment is related to the change of the near-surface Pb composition or to preferential Pb sputtering.[32] In this work, we separate both effects in order to clarify the Pb composition at the surface and in the bulk of the PLT films. On the basis of this analysis, we discuss the origin of the near-surface Pb enrichment.

A Y-stabilized zirconia (YSZ; $a = 5.14$ Å) buffer layer between PLT ($a = 3.93$ Å and $c = 4.05$ Å, for $x = 0.08$) and InP ($a = 5.8687$ Å) was used to decrease the PLT/InP lattice mismatch, as was already successfully proven for similar modified-$PbTiO_3$ systems.[34] This buffer also provides a diffusion barrier[35] and avoids InP degradation by oxidation[36] or phosphorus evaporation.[37] Attention is paid to diffusion processes at the PLT/YSZ and YSZ/InP interfaces.

Experimental Section

The YSZ and PLT films were sequentially deposited by PLD on monocrystalline (100)InP:Fe. A pulsed KrF excimer laser ($\tau = 16$ ns and $\lambda = 248$ nm) was used at a laser fluence of $J = 3$ J/cm^2 and a frequency of $\nu = 10$ Hz. The InP substrate was placed opposite the target at a distance of 60 mm. Details of the deposition procedures including the substrate preparation were reported elsewhere.[15,38]

To avoid InP oxidation, YSZ growth was performed in high vacuum (8×10^{-7} mbar) using YSZ, $x = 0.1$, targets and heating the substrate in the 550−600 °C range. Under these conditions, YSZ films with the epitaxial relationship ⟨100⟩{100}YSZ//⟨100⟩{100}InP and a low average roughness of, namely, 1 nm for 150 nm thick films were obtained at a rate of 0.1 Å/pulse.[38]

The PLT film was deposited on the YSZ buffer layer using a laser fluence of $J = 4-5$ J/cm^2 and a substrate temperature $T_s = 600-650$ °C. During deposition, molecular oxygen of high purity (99.999%) was introduced until the dynamic pressure of 0.1 mbar was reached. The ceramic target was prepared by solid-state reaction of a $PbO/La_2O_3/TiO_2$ mixture. The mixture was first dried at 120 °C and then uniaxially pressed at 3 kN/cm^2. The resulting pellet was heated for 24 h in an atmosphere enriched in Pb vapor at 1200 °C in order to eliminate carbon contamination and to promote the reaction. The pellet was milled, and the phases present were tested by X-ray diffraction (XRD). When single-phase $Pb_{0.88}La_{0.08}TiO_3$ material was achieved, the pellet was 10% weight-enriched in PbO to compensate the expected Pb loss. Therefore, the molar composition of the target is $Pb_{1.01}La_{0.08}TiO_{3.13}$. This mixture was uniaxially pressed at 3 kN/cm^2, isostatically pressed at 20 kN/cm^2, and finally sintered at 1250 °C.

The crystallinity and orientation of the films were studied by XRD with a D-500 Siemens diffratometer in standard $\theta-2\theta$ scans, using Cu Kα radiation. The thicknesses of the YSZ and the PLT layers were measured with a Talysurf-50 profilometer.

The RBS data were collected at a 3.1 Van der Graaf accelerator with a 1.6 MeV He$^+$ beam. Backscattered ions were detected by two surface barrier detectors of 12 and 18 keV energy resolution, at 180° and 140° to the beam direction, respectively. The simulation of the RBS spectrum was performed with the RUMP software.[39]

(20) Cotell, C. M.; Grabowski, K. S. *MRS Bull.* **1992**, *17* (2), 44.
(21) Martín, M. J.; Mendiola, J.; Zaldo, C. *J. Am. Ceram. Soc.* **1998**, *81* (10), 2542.
(22) Ishida, M.; Tsuji, S.; Hamawaka, Y.; Nakagawa, T. *J. Appl. Phys.* **1978**, *21*, 339.
(23) Horwitz, J.; Grabowski, S. K.; Chrisey, S. D. B.; Leuchtner, R. E. *Appl. Phys. Lett.* **1991**, *59* (3), 1565.
(24) Song, Z.; Ren, W.; Zhang, L.; Yao, X.; Lin, C. *Thin Solid Films* **1999**, *353* (1), 25.
(25) Ibuki, S.; Nakayawa, T.; Okuyama, M.; Hanakawa, Y. *Jpn. J. Appl. Phys.* **1990**, *29* (3), 532.
(26) Quian, Z. H.; Xiao, D. Q.; Zhu, J. G.; Li, Z. S. *J. Appl. Phys.* **1993**, *74* (1), 224.
(27) Yoon, S. G.; Park, J. D.; Choi, J. H.; Kim, H. G. *J. Vac. Sci. Technol. A* **1991**, *9* (1), 281.
(28) Dana, S. S.; Etzold, K. F.; Clabes, J. *J. Appl. Phys.* **1991**, *69* (8), 4398.
(29) Calzada, M. L.; Martin, M. J.; Ramos, P.; Mendiola, J.; Sirera, R.; Da Silva, M. D.; Soares, J. C. *J. Phys. Chem. Solids* **1997**, *58* (7), 1033.
(30) Lu, C. J.; Kuang, A. X.; Huang, G. Y. *J. Appl. Phys.* **1996**, *80* (1), 202.
(31) Chaoui, N.; Millon, E.; Muller, J. F.; Ecker, P.; Bieck, W.; Migeon, H. N. *Appl. Surf. Sci.* **1999**, *138* (Jan), 265.
(32) Sirera, R.; Leinen, D.; Rodríguez-Castellón, D. E.; Calzada, M. L. *Chem. Mater.* **1999**, *11* (11), 3437.
(33) Leinen, D.; Fernández, A.; Espinós, J. P.; Gonzalez-Elipe, A. R. *Surf. Interface Anal.* **1993**, *20*, 941.
(34) Horii, S.; Yokoyama, S.; Nakajima, H.; Horita, S. *Jpn. J. Appl. Phys., Part 1* **1999**, *38* (9B), 5378.
(35) Liu, J. M.; Xu, S. Y.; Zhou, W. Z.; Jiang, X. H.; Ong, C. K.; Lim, L. C. *Mater. Sci. Eng., A* **1999**, *269* (1), 67.
(36) Hollinger, G.; Bergignat, E.; Joseph, J.; Robach, Y. *J. Vac. Sci. Technol. A* **1985**, *3* (6), 2082.
(37) Farrow, R. F. C. *J. Phys. D* **1974**, *7*, L121.
(38) Vasco, E.; Vazquez, L.; Aguiló, M.; Zaldo, C. *J. Cryst. Growth* **2000**, *209* (4), 883.
(39) Doolite, L. R. *Nucl. Instrum. Methods Phys. Res.* **1985**, *B9*, 334.

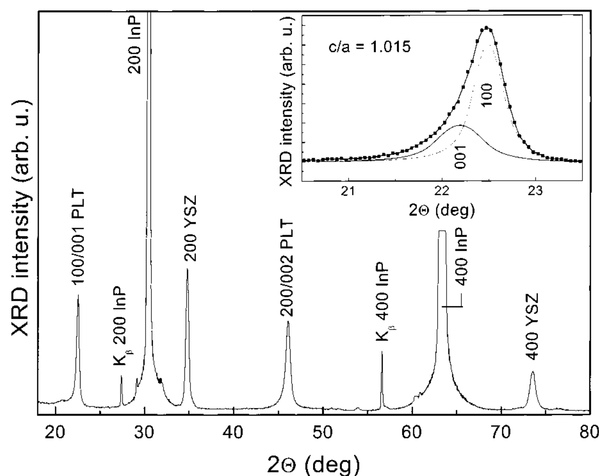

Figure 1. $\theta-2\theta$ XRD scan of a PLT/YSZ/(100)InP sample. The inset shows the deconvolution of the 100/001 PLT X-ray reflection by using two pseudo-Voight functions.

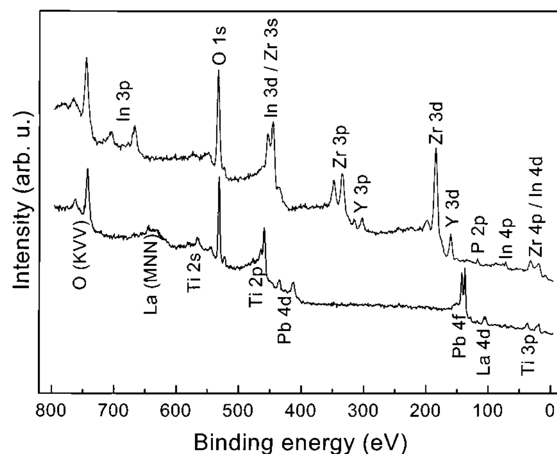

Figure 2. Survey XPS spectra taken at the PLT region (bottom spectrum) and at the YSZ/InP interface (top spectrum).

The XPS (Mg Kα) measurements were performed in an ultrahigh-vacuum chamber with a base pressure of 1×10^{-10} mbar, using a Perkin-Elmer ESCA/Auger spectrometer with a double-pass cylindrical mirror analyzer. The narrow scan spectra were taken at an analyzer pass energy of 50 eV, providing a resolution of 1 eV. Before the XPS data were analyzed, the contribution of the Mg $K\alpha_{3,4}$ satellite lines were subtracted and the spectra were subjected to a background subtraction formalism.[40] The atomic sensitive factor of each element was calculated using tabulated photoionization cross sections,[41] the free mean path of the emitted electrons,[42] and a transmission function of $1/E_{\text{kinetic}}$.[43]

The deconvolution of the Ti 2p and Pb 4f peaks was performed using Gaussian doublets with a spin−orbit split of 5.7 and 4.9 eV, respectively. The fit with Gaussian functions is justified, in our case, because of the limited resolution factor (≈1 eV) of the energy analyzer. Intensity ratios of 3:4 for the Pb $4f_{5/2}$ to Pb $4f_{7/2}$ contributions and 1:2 for the Ti $2p_{1/2}$ to Ti $2p_{3/2}$ were used. The energy range was calibrated using a pure gold standard as the reference.[44] To correct sample charging effects, the energy offset was permanently tested, using the Ti $2p_{3/2}$ peak (458.6 eV) as the reference.[26,27,30,33]

Depth profiling was performed with 3 keV argon ions over an area of 6×10 mm^2 with a total current of 0.5 μA for the first 20 nm and 4 μA for the rest of the sample depth. In a first approximation, when the influence of different materials and compositions on the sputter rate was neglected, the average sputter rate was previously estimated to be about 0.1 nm/μA·min.[45] The depth resolution of the profiling is limited by the lateral inhomogeneity of the ion etching process. It was measured (at a sharp interface at a depth of 1 μm) to be around ±5% of the respective depth.

Results

A. XRD Analysis. A [100/001]-oriented PLT was deposited on (100)YSZ/(100)InP. The corresponding XRD spectrum is shown in Figure 1. The PLT orientation was improved by the use of a YSZ buffer layer which reduced the lattice mismatch from 32% to 20%. Within the angular range of 20−80°, the XRD spectrum reveals only PLT 100/001 and its harmonic diffractions, without any other peak except the characteristic diffractions corresponding to the single-crystal buffer film and the substrate. The asymmetry of the 100/001 PLT peak is shown in the inset of Figure 1 and corresponds to the coexistence of two domains: an *a*-oriented domain, which is responsible for the 100 diffraction, and a *c*-oriented 001 domain. The 100/001 PLT peak was deconvoluted into 001 and 100 diffraction peaks using pseudo-Voight functions. The ratio between the intensities of the 100 and 001 X-ray diffractions was about $I_{001}/I_{100} = 0.35$, which is close to the ratio measured in the target ($I_{001}/I_{100} = 0.39$). This gives evidence of the nonprevalence of any domain. The obtained film tetragonality ($c/a = 1.015$) is lower than that in the target ($c/a = 1.033$). This is mainly due to the stress in the film/buffer interface, which tends to enlarge the *a* lattice parameter in order to reduce the free interface energy and the lattice mismatch. In addition, a La enrichment (with regard to the target composition) helps the cell to spread to be cubic.

B. XPS Analysis. The composition of the PLT/YSZ/InP samples has been analyzed at different depths by XPS. To achieve different sample depths, the film was eroded by Ar^+ bombardment. The sputter time has been converted into removed film thickness using the experimental calibration of the Ar^+ sputter rate. Prior to the analysis, the carbon contamination from the environment was removed by a slight (10 min with 0.5 μA) Ar^+ ion bombardment. Figure 2 shows surveys of the XPS spectra of the bulk PLT layer and the YSZ/InP interface. The relative amount of each element was calculated from the area of the XPS peaks obtained by narrow scans with high resolution. In the analysis of the PLT layer, two narrow scans including O 1s, Ti 2p, and Pb 4d peaks or Pb 4f and La 4d peaks were measured. For the analysis of the buffer layer and substrate, also two high-resolution scans were made including O 1s, In 3d, Zr 3s, Zr 3p, and Y 3d or Zr 3d, Y 3d, and P 2p.

Figure 3 shows the XPS composition profile of a PLT/YSZ/InP sample. The PLT and YSZ thicknesses obtained from the XPS depth profiles and the results obtained by profilometry (namely, 300 nm for PLT and 150 nm for YSZ) agree. Far from the surface and the interface regions, the composition of the different layers is constant. The composition of the PLT film deduced

(40) Shirley, D. A. *Phys. Rev B* **1972**, *5* (12), 4709.
(41) Scofield, J. H. *J. Electron Spectrosc. Relat. Phenom.* **1976**, *8*, 129.
(42) Seah, M. P.; Dench, W. A. *Surf. Interface Anal.* **1979**, *1*, 2.
(43) Briggs, D.; Seah, M. P. *Practical Surface Analysis*; John Wiley and Sons: Chichester, U.K., 1988.
(44) Fuggle, J. C.; Kallne, E. L.; Watson, M.; Fabian, D. J. *Phys. Rev. B* **1977**, *8* (2), 759.
(45) Böhme, O.; Cebollada, A.; Yang, S.; Teer, D. G.; Albella, J. M.; Román, E. *J. Appl. Phys.* **2000**, *88* (4), 1861.

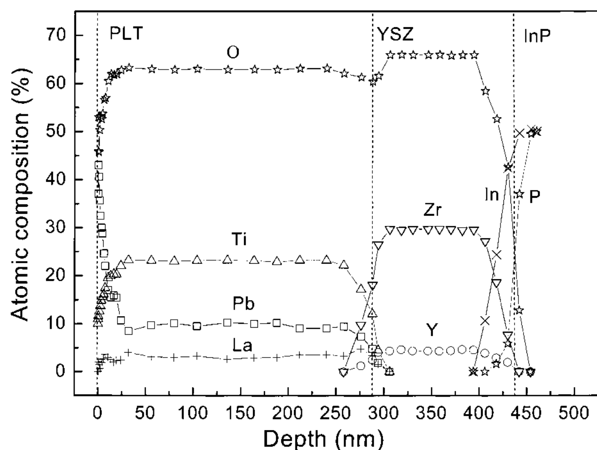

Figure 3. Percentage composition profile of a PLT/YSZ/(100)-InP sample obtained from the XPS results.

from these measurements is $Pb_{0.45}La_{0.12}TiO_{2.7}$. This would imply a tetragonal $Pb_{0.82-y}La_{0.12}TiO_{3-z}$ phase with huge fractions of Pb (y = 0.37) and O (z = 0.30) vacancies. The composition of the YSZ buffer layer was $Y_{0.13}Zr_{0.87}O_{1.94}$, similar to that of the YSZ target. Finally, the composition of the InP substrate was in the stoichiometric ratio.

The PLT/YSZ and YSZ/InP interfaces have a width (depth difference corresponding to 10−90% of the Zr saturation composition) of about 30 nm. These widths are of the same order as the depth resolution of the profiling process (i.e., 10% of the removed thickness). Thus, the inner interfaces of the multilayer system are abrupt without large interdiffusion. Only a slight 10−15 nm interdiffusion of In and O was detected.

The analysis of the top region of the PLT layer requires further detail. The film surface is predominantly composed of Pb and O in a ratio ≈ 5:6, while the composition of the other elements is depleted. The question is whether these changes are related to preferential sputtering processes or to real composition changes in the sample. To address this problem, two eroding regimes (different Ar^+ sputtering currents) were applied: First, to minimize any eventual preferential sputtering, the eroding was made with a sputter current of 0.5 μA. This regime was maintained until a nearly constant composition was reached. For the remaining depth profiling, the sputter current was raised to 4 μA.

Figure 4 shows the Pb/Ti, La/Ti, and O/Ti ratios obtained by XPS in the PLT near-surface region. The Pb/Ti and O/Ti ratios strongly decrease in the first 10 nm, whereas the La/Ti ratio, after an abrupt raise, remains constant. From 10 to 20 nm all of these ratios tend to saturation at the following ratios: Pb/Ti = 0.75, La/Ti = 0.12, and O/Ti = 2.94. This corresponds to a $Pb_{0.82-y}La_{0.12}TiO_{3-z}$ composition with y = 0.07 and z = 0.06. When the sputter current was increased, the La/Ti ratio remains constant but the lead and oxygen compositions fall to Pb/Ti = 0.45 and O/Ti = 2.7. These results evidence the preferential sputtering of Pb and O but, on the other hand, indicate the magnitude of these processes. We will further consider these results in the Discussion section.

C. Chemical Bonding Analysis. Figure 5 shows high-resolution XPS spectra, which reveal the chemical environment of the Pb, Ti, and O peaks along the

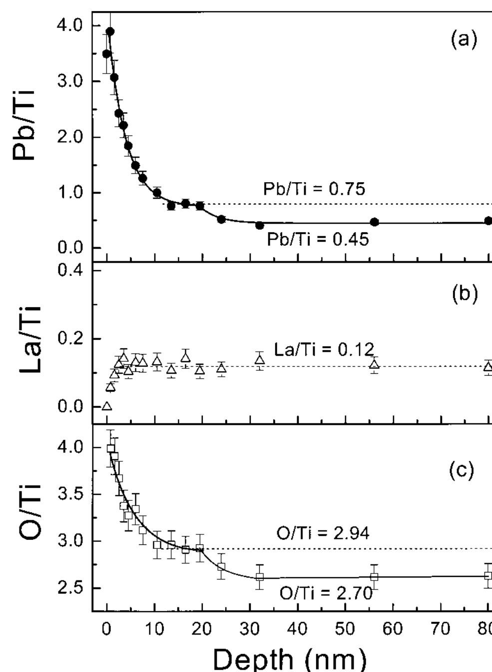

Figure 4. Atomic ratios near the surface of a PLT/YSZ/(100)-InP film: (a) Pb/Ti; (b) La/Ti; (c) O/Ti. Below 20 nm of film removal, the sputter density current was 0.83 μA/cm^2, and beyond this thickness, the density current was 6.7 μA/cm^2.

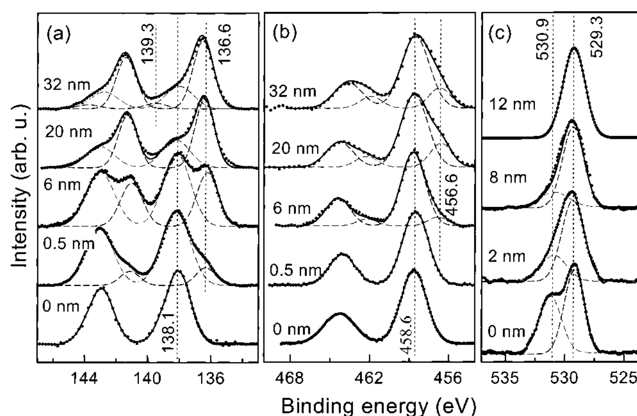

Figure 5. Evolution of the XPS spectra with the depth profiling by 3 keV Ar^+ sputtering: (a) Pb 4f XPS spectra; (b) Ti 2p XPS spectra; (c) O 1s XPS spectra. The points are the experimental results. Dashed lines are the Gaussian components used to fit the spectra, and the solid line is the convolution of the Gaussian components.

eroding process. The strongly overlapped La 4d doublet (not shown here), which appears after removal of the first 4 nm of the film at a binding energy of 102.6 eV, did not change its form along the eroding process.

The XPS spectra of Figure 5a show the $4f_{5/2}$ (higher binding energy side) and $4f_{7/2}$ (lower binding energy side) peaks of the Pb 4f doublet. At the PLT surface (0 nm spectrum), a symmetric $4f_{7/2}$ peak with a binding energy of 138.1 eV was measured. This peak can be ascribed to Pb^{2+} in the PLT phase[27,30,33] as well as to oxygen chemisorbed on lead (PbO_{ads}).[26] Both contributions cannot be distinguished because their energy separation (<0.4 eV) is below the resolution limit of our measurements. With proceeding depth profiling, the Pb 4f peaks develop shoulders at the low binding energy side (136.6 eV for $4f_{7/2}$); these shoulders correspond to the reduction of Pb^{2+} to metallic lead (Pb^0), likely

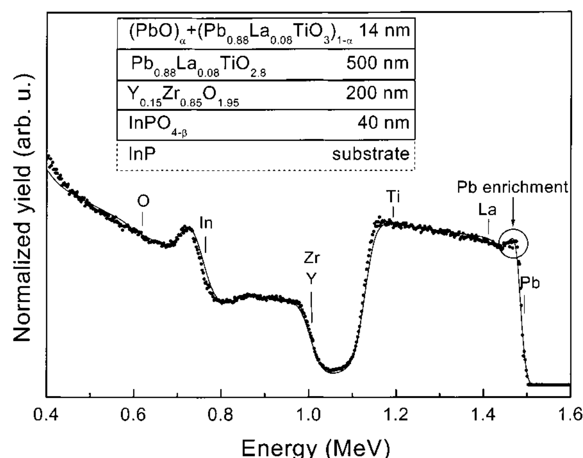

Figure 6. RBS spectrum of a PLT/YSZ/(100)InP sample. The points are the experimental results, and the line is the simulation obtained assuming the layer distribution indicated in the inset. The energy of the backscattered He^+ ions corresponding to each element on top of its layer is indicated.

induced by the molecular oxygen loss.[33] Finally, after the sputter current is raised to 4 μA, a third component at higher binding energy (139.3 eV) was created (32 nm spectrum). This latter contribution has also been observed by other authors in $PbTiO_3$[30] and is ascribed to ions (Pb^{2+}) which are isolated in the oxide dielectric matrix and are produced by long-term Ar^+ sputtering in ultrahigh vacuum.

The $2p_{1/2}$ (higher binding energy side) and $2p_{3/2}$ (lower binding energy side) contributions of the Ti 2p doublet in Figure 5b also show an evolution with the sputter time. At the surface (0 nm), the $2p_{3/2}$ peak is symmetric with a maximum at 458.6 eV. This binding energy corresponds to Ti^{4+} in $PbTiO_3$-modified phases.[26,27,30,33] With increasing depth, the XPS peaks broaden at the low binding energy side. This is ascribed to the reduction of Ti^{4+} to Ti^{3+} (456.6 eV).[33] However, the increase of the contribution of components attributed to lower oxidation species (e.g., Ti^{3+} and Pb^0) is slower in the Ti 2p doublet than in the Pb 4f.

At the PLT surface (0 nm), the O 1s singlet shown in Figure 5c is evidently a composed peak. Two Gaussian contributions at 529.3 and 530.9 eV have been used to fit the experimental spectrum. The component at higher binding energy decreased with the sputtering, while the intensity of the low binding energy component (529.3 eV) remains constant. This latter component was assigned to O incorporated in the PLT perovskite phase, in agreement with previous results.[26] The XPS peak at 530.9 eV corresponds to PbO_{ads}.[46] It should be stressed that this component is not due to any surface contamination. The spectrum designated with 0 nm in Figure 5c represents the as-received surface after a short ion cleaning, which is excluded from the depth axis. A third component at about 532.0 eV (not shown here) was removed by this ion cleaning process and is connected with surface contamination.

D. RBS Analysis. Figure 6 shows an RBS spectrum (points) of a PLT/YSZ/InP sample. The slight rise of the RBS signal on the high-energy side (about 1.47 MeV) reveals the existence of a thin layer predominantly composed of lead in a phase with a higher density than PLT. To test the reliability of the different experimental methods, the simulation (continuous line) of the RBS spectrum has been performed by taking into account the composition profile conclusions obtained by XPS and sketched in Figure 6. This includes an outermost Pb-rich layer (PbO_α + $PLT_{1-\alpha}$), uniform PLT and YSZ layers, and an oxidized InP region above the InP substrate. The difference between the thickness estimated from the RBS measurements and that estimated from XPS or profilometry is due to the uncertainty in the determination of the real film density made by the RBS evaluation program. For oxides, this normally leads to an overestimation of the thickness obtained from RBS.

Discussion

It should be noticed that, apart from the possible composition deviations at the film surface and at the buffer or substrate interfaces, the PLT and YSZ layers exhibit a uniform composition without significant interdiffusion (Figure 3). The composition of the YSZ layer is in agreement with the target composition used. However, it is clear that the absolute composition of the PLT layer obtained from XPS results depends on the experimental conditions of the Ar^+ sputtering process. Even though the energy (3 keV) and highest sputter current density (4 $\mu A/0.6\ cm^2 = 6.7\ \mu A/cm^2$) used in this work are lower than those used in previous XPS analyses,[25,33] the $Pb_{0.45}La_{0.12}TiO_{2.7}$ composition derived from XPS measurements under these sputtering conditions is not reliable because of the high Pb and O losses, which would imply the formation of the nonferroelectric $PbTi_3O_7$ pyrochlore phase.[29] This is in disagreement with our XRD results (Figure 1), which demonstrate that the film bulk is formed mainly of PLT tetragonal perovskite. This discrepancy is often attributed to the preferential removal of Pb and O ions induced by the Ar^+ sputtering.

Figure 4a shows two Pb composition regions, which correspond to the profiling regimes before and after of the change of the sputter conditions, respectively. In the first 12 nm underneath the film surface before the onset of a region with uniform Pb composition, the Pb loss is about 80% of the composition at the film surface. When the sputter current was enhanced by 8 times at 20 nm depth, the Pb loss is only 40% of the preceding value. This experiment clearly demonstrates that the Pb preferential sputtering is insufficient to cause the huge Pb loss in the first regime. It must be concluded that the intensity decrease of the XPS signals is indeed related to a depletion of the Pb composition accompanied by the preferential sputtering; i.e., the film surface is Pb-rich. This conclusion agrees with the chemical studies summarized in Figure 5c. The near-surface region of the film is composed of a mixture of $PbTiO_3$ (without La) and PbO_{ads}.

Our results of Figure 4 show that, in using a very low (0.5 $\mu A/0.6\ cm^2 = 0.83\ \mu A/cm^2$) sputter current density, the PLT film composition saturates at the nominal $Pb_{0.75}La_{0.12}TiO_{2.94}$ composition. This composition implies a $Pb_{0.82-y}La_{0.12}TiO_{3-z}$ phase with only minor Pb ($y = 0.07$) and O ($z = 0.06$) composition deviations. These

(46) Kim, K. S.; O'Leary, T. J.; Winograd, N. *Anal. Chem.* **1973**, *45* (13), 2214.

deviations still might be related to the preferential removal of Pb and O, induced by our sputter conditions. So, in a first approximation, 5−10% of Pb is lost because of preferential sputtering in the first eroding regime, and the surface is 70−65% Pb enriched with regard to the PLT film bulk.

Using the results of bulk ceramics,[47] the film tetragonality obtained in Figure 1, $c/a = 1.015$, implies a La/Ti = 0.18 ratio in the film. This value is not very far from the La/Ti = 0.12 ratio obtained by our XPS measurements. The difference may be due to stress in the film. In fact, much larger c/a shifts have been observed in sol−gel-prepared PLT films for the same La/Ti ratio.[48] The slight La/Ti ratio enhancement of the film (0.12) with regard to the target (0.08) might be attributed to the scattering of the ablated species in the oxygen-rich deposition atmosphere. This scattering becomes more important to light elements, such as Ti, and may modify the La/Ti ratio of the film.

A first approach to the chemical phases present in the near-surface region of the PLT film can be made by combining the element ratio (Figure 4) and the information of their chemical states (Figure 5). The constant La/Ti ratio and their chemical environments suggest that both elements only exist in the PLT form. However, the Pb/Ti and O/Ti ratios do not correspond to PLT stoichiometry, and consequently other lead- and oxygen-rich phases (lead oxide) should coexist. This coexistence explains the Pb/O ratio (≈5:6) and the depletion of other elements measured on the sample surface (Figure 3). While the small energy separation impedes one to distinguish PLT and PbO_{ads} in the Pb 4f spectra, the deconvolution of O 1s singlets reveals the existence of PbO_{ads}. Once this region was removed, the stabilization values of the Pb/Ti and O/Ti ratios in the first eroding regime (0.75 and 2.94, respectively) can be mainly attributed to PLT.

A final test for the reliability of the surface Pb enrichment is provided by the successful fit of the RBS spectrum in Figure 6 with a layer stacking, which includes a first thin (≈14 nm) Pb-rich layer formed by the $(PbO_{ads})_\alpha + (PLT)_{1-\alpha}$ mixture.

The $(PbO_{ads})_\alpha + (PLT)_{1-\alpha}$ mixture composition changes as a function of the film depth [i.e., $\alpha = f(\text{depth})$]. This relationship can be independently calculated from the Pb/Ti ratio or independently from the O_{PbOads}/O_{PLT} peak areas, taken from the O 1s resolved spectra. As is shown in Figure 7, the composition profiles obtained by the two ways agree. The PbO_{ads} fraction diminishes below the film surface linearly with the film depth at a rate of 6%/nm. The delay in the reduction of Ti^{4+} to Ti^{3+} compared to the reduction of Pb^{2+} to metallic Pb is connected with the mixture composition profile. Because the Ti oxidation state is only connected with the oxygen associated to PLT, the Pb^{2+} reduction without a corresponding Ti^{4+} reduction is only possible in the PbO_{ads} fraction.

The origin of the surface lead enrichment of $PbTiO_3$-modified films is controversial. Some authors attribute this effect to intrinsic phenomena related to the thermal cycling of the deposited material rather than to the deposition process.[26,28] This hypothesis is supported by the experimental observation of Pb-rich surfaces in films deposited by the different deposition techniques mentioned in the Introduction. However, stoichiometric and even lead-deficient surfaces in $PbTiO_3$-modified films deposited by sol−gel have also been reported.[30,32,49] Our results reveal that the Pb enrichment detected in the near-surface region neither can be explained as results of a lead preferential sputtering process nor can be extended to thermal-induced Pb diffusion from the film bulk to the surface. In our opinion, its origin in films deposited by physical vapor deposition techniques, such as PLD or sputtering, is closely linked to dynamic processes of Pb excess segregation, involved in the crystallization of the stoichiometric PLT film bulk.

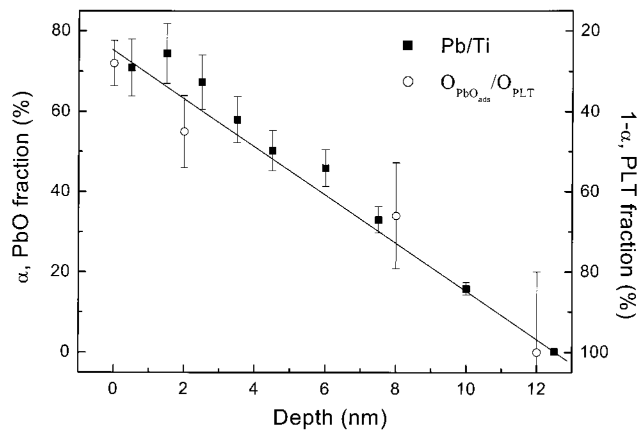

Figure 7. Evolution of the $(PbO_{ads})_\alpha + (PLT)_{1-\alpha}$ mixture composition with the film depth. The symbols are the experimental results, and the line corresponds to the fit obtained by considering $\alpha(\text{depth}) \propto -m \times \text{depth}$ (with m = 6%/nm).

The presence of a narrow InP oxide layer must be finally remarked in the YSZ/InP interface, which is ascribed to $InPO_4$, as revealed by the RBS simulation (Figure 6). Its formation is stimulated by the PLT deposition conditions: The high oxygen pressure used during the PLT deposition together with the fast ionic conductivity of the YSZ film[48,51] is the most likely oxygen source for this InP reoxidation. It must be concluded that the YSZ buffer acts well as a stable barrier to PLT/InP interdiffusion. Taking into account the widths of the PLT/YSZ and YSZ/InP interfaces, a first estimation reveals that a 80 nm YSZ film is sufficient to act as a buffer layer in this system.

Conclusions

Reliable composition profiles of the constituent elements of PLT films can be achieved by minimizing the Ar^+ sputtering power used for film eroding below 3 keV and 1 $\mu A/cm^2$. Under our experimental deposition conditions, a Pb-rich region is formed in the outermost 10−20 nm of the film. This region is composed of a mixture of oxygen-chemisorbed lead (PbO_{ads}) and a La-depleted

(47) Yamamoto, T.; Igarashi, H.; Okazaki, K. *J. Am. Ceram. Soc.* **1983**, *66* (5), 363.
(48) Wang, J. P.; Chen, Y.; Lee, M. C. *Jpn. J. Appl. Phys., Part 1* **1998**, *37* (3A), 951.
(49) Leinen, D.; Sirera, R.; Rodríguez-Castellón, E.; Calzada, M. L. *Thin Solid Films* **1999**, *354* (1), 66.
(50) Fenner, D.; Viano, A.; Fork, D.; Connell, G.; Boyce, J.; Ponce, F.; Tramontana, J. *J. Appl. Phys. Lett.* **1991**, *69* (4), 2176.
(51) Tarsa, E. J.; McCormick, K. L.; Speck, J. S. *Mater. Res. Soc. Symp. Proc.* **1994**, *341*, 73.

PLT. The mixture composition changes linearly with the film depth below the film surface.

YSZ is a good buffer to integrate PLT on InP. A 80 nm or even thinner YSZ layer is sufficient to minimize PLT/InP interdiffusion and deep substrate reoxidation. Thanks to the ⟨100⟩{100}YSZ||⟨100⟩{100}InP epitaxy, the PLT layer is preferentially oriented with the [100] and [001] PLT directions parallel to the [100] InP one.

Acknowledgment. This work has been supported by CICyT (MAT99-1077 and CAM (07T/0032/1997) projects as well as by a CSIC (Spain)−ICCTI (Portugal) cooperation agreement. E.V. is supported by an AECI grant (Spain).

CM001198P